

Research on the Influence of Compressed Low Pressure Steam Blasting Treatment on the Chemical Composition of Explosives

Weilong An

Dongyu No. 30, Xisan Village, Huairou, Beijing, China.

Abstract

Aiming at the problem of insufficient supply of emulsified charge and restricting the progress of pre-splitting blasting, a new charge structure mode was explored, that is, a low-power porous granular ammonium explosive charge was axially continuous and radially uncoupled. Theoretical verification of the feasibility of the structure of the charge, and at the same time using the LS-DYNA software numerical simulation method, a 1:1 model was established against the actual aperture of the mine, and the difference between the uncoupled charge structure and the traditional emulsification drug volume was compared and analysed. It is concluded that the axial continuous charge of granular ammonium explosive has advantages in protecting the hole wall and crack propagation.

Keywords

Compression Low Pressure; Steam Explosion Treatment; Explosive Chemistry.

1. Introduction

Smooth blasting technology, as one of the controlled blasting technologies, emerged in Sweden in the 1950s. After being introduced to China in the mid-1960s, it has been widely used in mines, tunnels and slope engineering. Some scholars introduced the calculation principles of the main parameters of smooth blasting and guided on-site application. Some scholars proposed a calculation method for smooth blasting parameters under the influence of damage factors for weak and broken rock masses, and conducted field tests to verify them. Since the 1950s, bulk explosives, mainly ammonium explosives and emulsion explosives, have been widely used. At present, bulk emulsion explosives are widely used in roadway driving and blasting, and there are relatively few reports on the application of granular ammonium explosives in roadway driving in China. Based on the analysis of the original conditions of blasting in the copper mine and the existing problems in roadway excavation, this paper obtains the charge and hole distribution parameters of smooth blasting through calculations, and refers to the use of granular ammonium explosives in roadway excavation at home and abroad [1]. The field application test research and promotion of ammonium explosives in the copper mine has achieved the purpose of reducing costs and increasing efficiency, and achieved good economic and social benefits. It is also a domestic

2. Air shock wave interacts with the blasthole wall

2.1 Basic assumptions

In the uncoupled charge blasting process, the explosive detonation process, the generation and propagation process of the air shock wave, the interaction process between the air shock wave and the blasthole wall are very complicated [2]. The arc surface of the blasthole wall causes the shock wave penetration and reflection superimposition effect, the detonation wave propagates along the axial direction under the initiation condition of the columnar charge blasting point, etc., which increase the difficulty of theoretically accurately calculating the peak pressure of the blast hole wall. In order to facilitate the study, the interface between the air shock wave and the blast hole wall is

simplified as a plane, and the blast hole wall is assumed to be an elastic wall, and the air shock wave is assumed to be incident on the interface. At the same time, the interaction between the air shock wave and the blast hole wall is simplified. It is a one-dimensional plane problem, that is, the influence of the detonation wave propagating along the axial direction on the peak pressure of the blasthole wall is not considered.

2.2 Expansion process of detonation products and shock wave propagation process

Considering the one-dimensional plane flow, the pressure distribution of the detonation wave propagating to the interface between the explosive and the air and the initial penetration into the air is shown in Figure 1. In the figure, p_0 is the initial pressure of the air, p_s is the pressure of the penetrating air, p_x is the pressure at the interface, and p_H is the detonation wave front pressure. Figure 1(a) shows the stage before the detonation wave is transmitted to the interface between the explosive and the air space; Figure 1(b) shows the stage after the detonation wave penetrates into the air space [3]. At this time, the detonation process has ended and the initial detonation The compressed air of the detonation product forms an initial air shock wave; at the same time, the incoming rarefaction wave in the detonation product reduces the pressure of the detonation product, and the interface velocity and pressure of the detonation product and air are u_x and p_x , respectively. The separation distance between the air shock wave and the detonation product is difficult to determine. During the blasting process of a spherical charge, the two will be separated at 10-15 times the charge radius. Therefore, for the cylindrical charge blasting with a small non-coupling coefficient, the air shock wave is not separated from the detonation products during the propagation process.

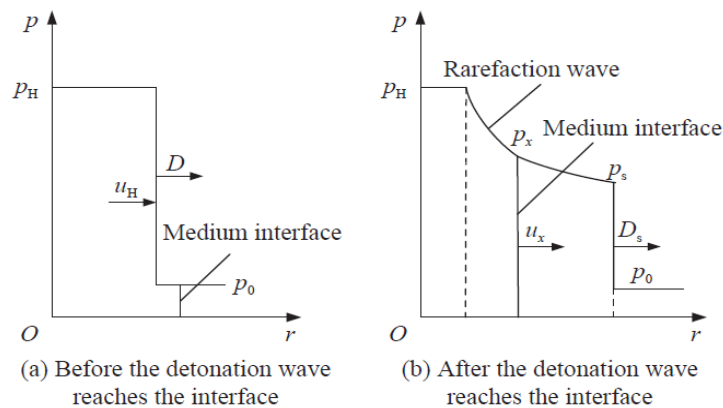


Figure 1. Pressure distribution before and after the detonation wave reaches the interface

Assuming that $p_{10}, \rho_{10}, u_{10}$ represents the pressure, density and velocity of the material after the air shock wave, $p_{20} = \rho_{20} = u_{20} = 0$ represents the original pressure, density and velocity of the rock mass respectively; ρ is the shock wave or sparse wave velocity propagated on the left, D_{x2} is the shock wave velocity propagated on the right; $p_{x1}, \rho_{x1}, u_{x1}$ is respectively The pressure, density, and velocity of the left interface, $p_{x2}, \rho_{x2}, u_{x2}$ is the pressure, density, and velocity of the right interface, respectively [4]. The following is an analysis of the interaction between air shock waves and elastic walls based on elastic theory and wave theory. The speed of the left interface can be calculated:

$$u_{x1} = u_{10} + \frac{2\gamma p_{10}}{(\gamma-1)\rho_{10}c_{10}} \left(1 - n_1^{(\gamma-1)/2\gamma}\right) \quad (1)$$

When the reflected wave formed in the material after the air shock wave is a shock wave, the particle velocity of the product after the shock wave is reduced from u_{10} to the moving speed u_{x1} of the left interface, and the product after the wave also obtains an additional velocity ur , which is equal to u_{x1} . The difference with u_{10} , namely:

$$u_r = u_{x1} - u_{10} = -\sqrt{(p_{x1} - p_{10})(v_{10} - v_{x1})} \quad (2)$$

In the formula: v_{10} is the specific volume of the detonation product, and v_{x1} is the specific volume of the material after the shock wave is reflected on the left side.

3. Blasting conditions

3.1 Number of blast holes and single-hole charge

In the smooth blasting design calculation, the blast holes of the tunnelling section from the centre to the periphery are: cut holes, reaming holes, auxiliary holes, and peripheral holes (top hole, side hole and bottom hole). Blasting adopts two large-hole straight hole cutting methods. The large cutting hole is formed by reaming the cutting hole with a reaming drill bit, with a diameter of 102mm and no charge. The roadway adopts one-time full-face excavation. For the roadway section, 41 blast holes need to be arranged, plus 2 cut holes, for a total of 43 blast holes. Among them, there are 8 cut holes (including 2 hollow holes), 4 reaming holes, 10 auxiliary holes, 15 top and help holes, and 6 bottom holes. The charge coefficient of each type of blasthole, the depth of the drill hole, the mass and length of the single volume of the charge used, and the blasting parameters calculated according to formula (1) are shown in Table 1. The blast hole layout of the tunnelling section is shown in Figure 2.

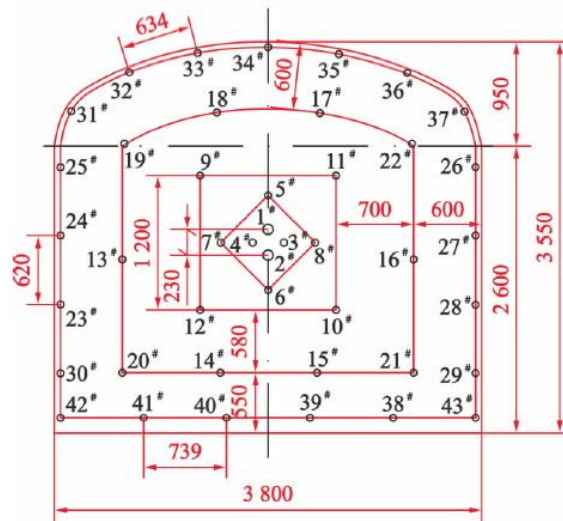


Figure 2. Schematic diagram of blasthole layout in tunnelling section

Table 1. Blasting parameters of tunnelling section

Blast hole number	1#-2#	3#-8#	9#-12#	13#-22#	23#-37#	38#-43#
Blast hole name	Empty hole	Cut hole	Reamed hole	Auxiliary hole	Help hole and top hole	Bottom hole
Hole depth/m	3.5	3.5	3.3	3.3	3.3	3.4
Charge coefficient	2	0.85	0.75	0.7	0.55	0.8
Number of holes		6	4	10	15	6
Number of rolls		6	5	4	6	5
Mass/kg		4.06	2.72	2.4	1.35	3.71
Total charge/kg		24.4	10.9	24	20.2	22.3
Initiation sequence		I	II	III	IV	V

3.2 Charge structure and blast hole blockage

The cut hole, reaming hole, auxiliary hole and bottom hole adopt continuous uncoupled charges; the top hole and side hole use air column spacing uncoupled charges, which are tied to the bamboo billet, and the detonating cord is connected for blasting [5]. All blastholes are blocked with the blasthole specially made by the blasthole machine, and the length of the blockage is not less than 0.4m.

4. Experimental results

4.1 Determination of the detonation velocity of mixed emulsion explosives

Perform 3 detonation velocity test tests on various emulsion explosives prepared, and take the average value of the detonation velocity. In order to facilitate the observation of the statistical results, a broken line chart of the average detonation velocity is drawn, as shown in Figure 3.

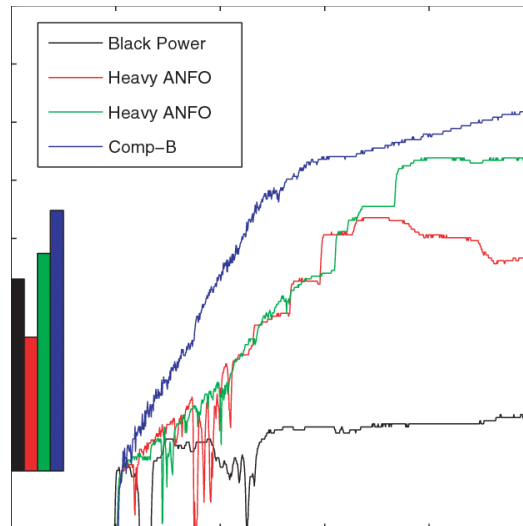


Figure 3. Comparison of the average detonation velocity of various types of emulsion explosives

While keeping the emulsifier ratio unchanged, diesel and engine oil are in a 3:1 ratio. When the burning oil accounts for 5%, the detonation velocity reaches the maximum value of 4476 m/s.

4.2 Analysis of blasting effect

After blasting, collect pictures of the explosion pile in time, use basketball as a reference, and use the fragmentation analysis software Split-Desktop4.0 to perform statistical analysis on the fragmentation of the explosion pile after blasting [6]. When analysing the fragmentation, set the relevant parameters in the software and process the collected pictures. According to the size of the site excavation and transportation equipment, the rock with the maximum diameter of more than 1.5m is called a large block. The overall effect of blasting is shown in Figure 4, and the statistics of bulk rate are shown in Table 2.

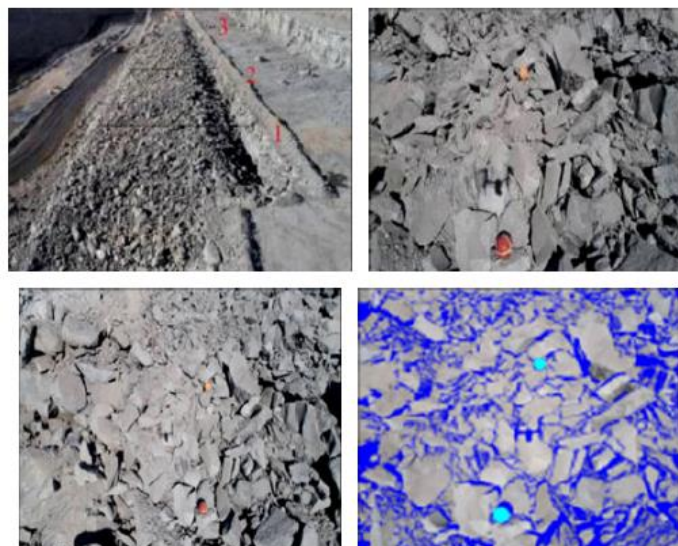


Figure 4. Blasting effect

It can be seen from Table 2 that the statistical summary of the blasting effect before and after the adjustment of the mixed explosive formula shows that: before the adjustment, the large block rate of the mine bench blasting was between 7.15% and 10.42%, and the average large block rate was 8.81%; after the adjustment, the large block rate of mine bench blasting is between 2.87% and 3.56%, and the average large block rate is 3.13%. After the adjustment of the mixed explosive formula, the blasting mass rate in mines has been reduced by 5.68% compared to before the adjustment. This effectively reduces the blasting mass rate and improves the overall construction efficiency of the mine stripping mining drill and blasting shovel shipment and transportation.

Table 2. Fragmentation statistical analysis

Test group	Proportion of various rock blackness/%<120cm	Bulk rate/%	Unit consumption/(kg·m ⁻³)
Additive Group A	88.95	92.8	7.2
Additive Group C	89.36	93.5	6.5
Original formula group	84.69	91.3	8.7

5. Conclusion

1) The application of smooth blasting technology has significantly improved the formation of the roadway. The phenomenon of over-under-excavation ($\pm 20\text{mm}$) has been reduced from 15% to 6%, and the average footage per shot has been increased from 2.7m to 3.0m, an increase of 11.1%, the hole mark rate of light blasting can reach more than 70%, which is more conducive to construction safety, but the use of rolled emulsion explosives for roadway excavation still has disadvantages such as high labour intensity and high cost. 2) Theoretical analysis and field test results show that granular ammonium explosives can be used for roadway blasting construction, saving charging time by more than 15% on a single working surface, and reducing the cost of direct explosives by US\$30.25. 3) The popularization and application of granular ammonium explosives in the tunnelling of the copper mine shows that the use of granular ammonium explosives can improve the working efficiency of workers and trolley equipment, reduce the cost of explosives, and achieve the purpose of reducing costs and increasing efficiency. Its successful experience is worth learning from other mines.

References

- [1] Kudo, S., Okada, J., Ikeda, S., Yoshida, T., Asano, S., & Hayashi, J. I. Improvement of pelletability of woody biomass by torrefaction under pressurized steam. *Energy & Fuels*, 33(11) (2019) 11253-11262.
- [2] Tanasă, F., Zănoagă, M., Teacă, C. A., Nechifor, M., & Shahzad, A. Modified hemp fibers intended for fiber-reinforced polymer composites used in structural applications—A review. I. Methods of modification. *Polymer Composites*, 41(1) (2020) 5-31.
- [3] Shu, B., Ren, Q., He, Q., Ju, Z., Zhan, T., Chen, Z., ... & Yangzhou, P. R. Study on mixed biomass binderless composite based on simulated wood. *Wood Research*, 64(6) (2019) 1023-1034.
- [4] Rosa, C. H. S., Mothe, M. G., Marques, M. F. V., Mothé, C. G., & Monteiro, S. N. Steam-exploded fibers of almond tree leaves as reinforcement of novel recycled polypropylene composites. *Journal of Materials Research and Technology*, 9(5) (2020) 11791-11800.
- [5] Debiagi, F., Madeira, T. B., Nixdorf, S. L., & Mali, S. Pretreatment efficiency using autoclave high-pressure steam and ultrasonication in sugar production from liquid hydrolysates and access to the residual solid fractions of wheat bran and oat hulls. *Applied biochemistry and biotechnology*, 190(1) (2020) 166-181.
- [6] Tienne, L. G., Cordeiro, S. B., Brito, E. B., & Vieira Marques, M. D. F. Microcrystalline cellulose treated by steam explosion and used for thermo-mechanical improvement of polypropylene. *Journal of Composite Materials*, 54(24) (2020) 3611-3624.